

## Authors' Response to Referee #2

We thank Referee #2 for the careful review and valuable comments and suggestions, which significantly contributed to improve the manuscript. All comments are addressed below.

### Anonymous Referee #2

Received and published: 16 December 2015

*Authors present a very interesting AMS (Aerosol Mass Spectrometer) data set obtained in two major cities in China (Xi'an and Beijing) during winter 2013/2014. The field campaign was characterized by 2 (or 3) extreme haze events with PM<sub>2.5</sub> concentrations up to 1000 µg/m<sup>3</sup>. During these haze events about 40% of the PM<sub>2.5</sub> mass concentration is in the 1-2.5 µm size fraction, which underscore the relevance of PM<sub>2.5</sub> aerodynamic lens inlet in such heavily polluted environments. The authors adopt a rigorous source apportionment strategy in order to reduce the subjectivity of the choices that must be done at different steps of the data treatment and to improve the representability of the solutions.*

*Overall the paper is well written, well-illustrated, the methodology is robust and the results present a real interest for the scientific community. One can just regret the lack of ancillary measurements such as offline chemical PM analyses (OC/EC, major ions) or SMPS/OPC measurements. This paper should be accepted on completion of the minor revisions/clarification requested below.*

**P30134 line 25.** *Clarify the position of the nafion drier (ie. in the 4 L/min primary line or after the split to the AMS line, not clear)? As RH can play an important role in terms of aerosol size distribution what was the RH after the nafion dryer during haze events?*

**Response:** The nafion drier was positioned after the split between the auxiliary flow and the AMS line. Unfortunately we couldn't calibrate our RH sensor. However, the recorded signal (in Volts) shows a constant signal, with no clear differences between the extreme haze events and the reference periods. In addition, aerosol sampling was conducted at room temperature, significantly higher than ambient temperatures, resulting for the extreme haze and reference periods in very low RH values in the line even prior to the drier. Therefore we are confident that the differences in the aerosol size distributions for the extreme haze and reference periods are not due to the different measurement RH in our case.

**Changes in text:** **After the split with the auxiliary flow and before entering the AMS**, the sampling air was drawn through a nafion drier in order to...

**P30135 line 10-20, comparison with offline gravimetric measurements.** *I'm surprised by the difference between offline gravimetric measurements and AMS+Aethalometer observed during the haze period which cannot be explained by "deposition of dust and waters on the filters"(remove). The samples were collected at ambient temperature or in heated shelter?*

**Response:** The filters were collected at ambient temperature. This information has been added in the revised manuscript. As mentioned in the text, the observed difference between offline gravimetric measurements and AMS+Aethalometer during extreme haze and reference periods can be due to differences in the size of the particle sampled. The AMS high pressure lens quantitatively transmits particles between 80nm and up to at least 3 µm. Comparatively, the effective cut-off diameter of the filter sampler inlet is at 2.5 µm (ideally a 50 % efficiency cut-off at 2.5 µm aerodynamic diameter). The particle transmission function for the offline sampler was not determined in our case, but may have not been very sharp resulting in losses of larger particles. We estimated that particles with aerodynamic diameters between 1 µm and 2.5 µm can contribute up to 40% of the total PM<sub>2.5</sub> mass during haze events. A loss of part of this mass in the offline sampler would explain the lower mass measured from gravimetric analysis compared to AMS. On average, gravimetric measurements have a negative bias of 24.7 %.

**Changes in text:**

Line 11: with gravimetric measurements on filters (collected also in the PM<sub>2.5</sub> range **at room temperature**).

**P30137 line 19.** *What is  $j$  in eq (3)?*

**Response:**  $j$  indicates the mass fragment fitted in high resolution.

**Changes in text:** “For example, in the case in which a factor profile ( $f_j$ , where  $j$  indicates the  $m/z$  of the ions fitted in high resolution) is constrained...”

**P30138 line 2:** *Among traffic sources, Diesel LDV/HDV are obviously the main BC emitter, but I suggest to change “diesel engines” by “traffic”.*

**Response:** We fully agree with the reviewer and have changed “diesel engines” with “traffic” in the revised manuscript.

**Changes in text:** “... can be distinguished from eBC emitted by traffic (eBC<sub>tr</sub>)...”

**P30138 line14-30 and P30139 first §.** *This section is very interesting and I suggest to go further in the discussion and to provide more details. Regarding the multilinear approach did the authors mix the two data sets (Xi'an and Beijing)? If yes, as coal could be quite different from one region to another, is there a difference in terms eBC/CCOA between the 2 cities (by applying the same methodology to each dataset separately)? Why did the authors choose to keep the results from the Aethalometer models instead of the results obtained from the multilinear approach which should provide the eBC contribution from coal combustion, fossil fuel combustion (derived from HOA) and wood burning?*

**Response:** This is an important point raised by the reviewer that requires some explanation. In Xi'an where the CCOA contribution was relatively low, the determination of eBC/CCOA from the multi-linear results was very uncertain. That is, several combinations of fitting parameters yielded a similar goodness-of-fit. This is because of the considerable correlation among the primary OA (POA) time series (due to the strong influence of the PBL dynamics) and the variability of the ratios between BC and POA for the different periods (as found from the Aethalometer model, table S1). Therefore, we chose to use the aethalometer model instead as a relatively independent method for the apportionment of eBC sources in Xi'an. A shortcoming of this model is that additional brown carbon from sources other than biomass burning, e.g. coal burning may lead to a misinterpretation of the results. As coal burning is a major source in Beijing, the multilinear results were more robust and hence could be used for the estimation of eBC/CCOA ratio. This ratio was then used to confirm that the contribution of coal burning to eBC is negligible for the case of Xi'an, supporting the application of the aethalometer model under these conditions. As the coals used in Beijing and Xi'an and their neighboring areas are a mixture of different coal types from Northern China, we consider reasonable the use of the eBC/CCOA from Beijing for analyzing the Xi'an dataset.

**P30139 line 8.** *Considering DeWitt et al 2015 (ACP) a ratio BC/HOA of 0.79 should correspond to a % of diesel fuel consumption of about 30-40%. Does this make sense in China?*

**Response:** We thank the reviewer for a very constructive comment. Although the car fleet in China is strongly dominated by gasoline powered vehicles, diesel fuel dominates the heavy and medium duty vehicles (i.e. trucks and buses). Therefore diesel account for ~40% of the total fuel consumed in 2013, as shown in Figure R1 (Gentner et al., in prep.).

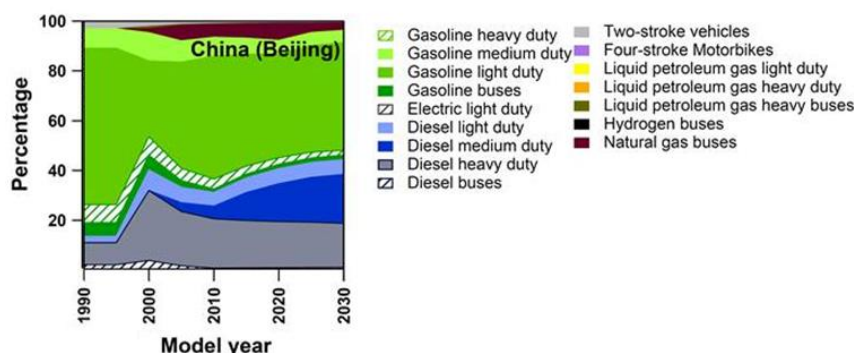


Figure R1: Figure modified from Gentner et al. (in prep.)

#### Changes in text:

The ratio  $eBC_{tr}$  to HOA was 0.79, which is lower than the ratios reported in previous European studies (El Haddad et al., 2013 and references therein) but is in good agreement with results derived from measurements in China (Huang et al., 2012; Zhou et al., 2014). This difference in the  $eBC_{tr}$  to HOA ratio at the two locations is most probably related to the higher percentage of gasoline vehicles in China compared to Europe. **Specifically, according to DeWitt et al. (2015), an  $eBC_{tr}$  to HOA of around 0.8 corresponds to a diesel fuel share of about 40 to 50 %. This estimation is in good agreement with results from Gentner et al. (in prep), where a diesel fuel share of around 40 % was estimated for 2013 in China, dominated by heavy and medium duty vehicles.**

**P30139.** PAH quantification. About half of the  $m/z$  listed are not molecular ions. Moreover as PAHs are a vast family of compounds (without considering alkylated PAHs nor oxygenated nor nitrated PAHs) and as the PAH concentrations reported here are very high (!) and one of the main point developed in the discussion, more details are necessary in this section. Especially it's important to establish a rough correspondence between the ions considered for the quantification and the PAHs or nitroPAHs (lot of common fragments between these two subfamilies). Such correspondences are not easy to get precisely and will be subjected to uncertainties, but it's important in order to compare with the literature and to fix the limits of the compounds actually quantified or not considered here in the quantification (again the PAH family is vast).

**Response:** We fully agree with the reviewer's comment and have added a discussion about possible errors related to the AMS-PAH quantification in the revised manuscript. PAH quantified from AMS measurements (which we will refer to as AMS-PAH) have been found to be systematically higher than PAH determined from filter measurements in previous works (Bruns et al., 2015). These differences were mostly attributed to filter artifacts (predominantly negative artifacts, i.e. volatilization of PAH on the filter surface). However, also the AMS-PAH analysis is subject to uncertainties. The PAH RIE considered in this work (1.4) is at the lower end of the values found in literature (e.g. Dzepina et al. (2007) measured RIEs between 1.35 and 2.1 for four PAH standards), and the reported PAH values would decrease by 33.3 % if a higher RIE (2.1) would be considered. Moreover, as pointed out by the reviewer, our results might be affected by interferences with fragments from other PAH classes at the quantified  $m/z$ 's. To assess the contribution of these interferences we have analyzed the electron impact ionization mass spectrum (Linstrom et al., 2016) of major PAHs derivatives including alkylated, oxygenated and nitro-PAHs (43 compounds in total). The fragmentation patterns of alkylated and oxygenated-PAHs suggests that their response at the  $m/z$ 's of interest is highly unlikely. On the other hand, nitro-PAHs exhibit a small response at some fragments of interest, but yield mainly fragments at odd  $m/z$ . The non-molecular ions (at odd  $m/z$ 's) have been removed from the list of molecular ions in the revised manuscript and are discussed separately at the end of the paragraph. These ions ( $[C_{11}H_7]^+$  (139),  $[C_{13}H_7]^+$  (163),  $[C_{13}H_9]^+$  (165),  $[C_{15}H_9]^+$  (189) and  $[C_{16}H_7]^+$  (199)) have been observed to derive from the fragmentation of PAHs using laser desorption (Bente et al., 2009); they contribute to 32% of the total PAH mass quantified here. Due to all the limitations mentioned above, PAHs' concentrations presented here have to be considered as absolute highest estimates and we will refer to this chemical family as AMS-PAHs.

#### Changes in text:

PAH concentrations were quantitatively determined from the high resolution AMS data. All details about the method used can be found in Bruns et al. (2015) and references therein. The following PAH molecular ions  $[M]^+$  were fitted in the HR spectra:  $[C_{10}H_8]^+$  (128),  $[C_{11}H_7]^+$  (139),  $[C_{12}H_8]^+$  (152),  $[C_{13}H_7]^+$  (163),

[C<sub>13</sub>H<sub>9</sub>]<sup>+</sup> (165), [C<sub>14</sub>H<sub>8</sub>]<sup>+</sup> (176), [C<sub>14</sub>H<sub>10</sub>]<sup>+</sup> (178), [C<sub>15</sub>H<sub>9</sub>]<sup>+</sup> (189), [C<sub>16</sub>H<sub>7</sub>]<sup>+</sup> (199), [C<sub>16</sub>H<sub>10</sub>]<sup>+</sup> (202), [C<sub>18</sub>H<sub>10</sub>]<sup>+</sup> (226), [C<sub>18</sub>H<sub>12</sub>]<sup>+</sup> (228), [C<sub>20</sub>H<sub>12</sub>]<sup>+</sup> (252), [C<sub>22</sub>H<sub>12</sub>]<sup>+</sup> (276), [C<sub>22</sub>H<sub>14</sub>]<sup>+</sup> (278), [C<sub>24</sub>H<sub>12</sub>]<sup>+</sup> (300) and [C<sub>24</sub>H<sub>14</sub>]<sup>+</sup> (302), with the nominal mass in parentheses. In addition to the aforementioned molecular ions, also other associated fragments were considered, including [M-H]<sup>+</sup>, [M-2H]<sup>+</sup>, [M]<sup>2+</sup> and [M-H]<sup>2+</sup> and the <sup>13</sup>C-isotopes of singly charged ions. To reduce uncertainty in the quantification of the associated ions, the ratios between molecular ions and their corresponding fragments were determined during periods with high PAH concentrations and then applied to the entire data set. **Due to possible interference with ions from non-PAH compounds, the fragments that presented low correlation with their corresponding molecular ions (i.e. R<sup>2</sup> below 0.6 for C<sub>13</sub>H<sub>6</sub> to C<sub>13</sub>H<sub>7</sub> and C<sub>16</sub>H<sub>6</sub> to C<sub>16</sub>H<sub>7</sub> ratios) were not taken into account in the analysis. In cases of overlap between a molecular ion and associated fragments (e.g. [M-2H]<sup>+</sup> from [C<sub>14</sub>H<sub>10</sub>]<sup>+</sup> overlaps with the molecular ion [C<sub>14</sub>H<sub>8</sub>]<sup>+</sup>) the fragments were not included.** As for the non-PAH organics, the RIE for PAHs was ~~assumed-considered~~ to be 1.4 and the dependency of the collection efficiency (CEb) on the chemical composition of the aerosol was estimated using a composition dependent collection efficiency (CDCE) algorithm (Middlebrook et al., 2012). **Previous works found that PAH quantified from AMS measurements were systematically higher than PAH determined from filter measurements (Bruns et al., 2015). These differences were mostly attributed to filter artifacts (predominantly negative artifacts, i.e. volatilization of PAH on the filter surface). However, also the AMS-PAH analysis is subject to uncertainties. The PAH RIE considered in this work (1.4) is at the lower end of the values found in literature (e.g. Dzepina et al. (2007) measured RIEs between 1.35 and 2.1 for four PAH standards), and the reported PAH values would decrease by 33.3 % if a higher RIE (2.1) would be considered. Moreover, our results might be affected by interferences with fragments from other PAH classes at the quantified *m/z*'s. To assess the contribution of these interferences we have analyzed the electron impact ionization mass spectrum (Linstrom et al., 2016) of major PAHs derivatives including alkylated, oxygenated and nitro-PAHs (43 compounds). The fragmentation patterns of alkylated and oxygenated-PAHs suggests that their response at the *m/z*'s of interest is highly unlikely. On the other hand, nitro-PAHs exhibit a small response at some fragments of interest, but yield mainly fragments at odd *m/z*. In addition to the molecular ions mentioned above, we have considered as PAHs the ions [C<sub>11</sub>H<sub>7</sub>]<sup>+</sup> (139), [C<sub>13</sub>H<sub>7</sub>]<sup>+</sup> (163), [C<sub>13</sub>H<sub>9</sub>]<sup>+</sup> (165), [C<sub>15</sub>H<sub>9</sub>]<sup>+</sup> (189) and [C<sub>16</sub>H<sub>7</sub>]<sup>+</sup> (199) and their related associated fragments. These fragments at odd masses have been observed to derive from the fragmentation of PAHs using laser desorption (Bente et al., 2009); they contribute to 32% of the total PAH mass quantified here. Due to all the limitations mentioned above, PAHs' concentrations presented here have to be considered as absolute highest estimates and we will refer to this chemical family as AMS-PAHs.**

**P30140-30145 Source apportionment Optimization (general).** *This section is undoubtedly the most innovative part of the paper. The methodology adopted by the authors to minimize the subjectivity of the solutions is scientifically robust and interesting from a conceptual point of view. My main question is what are the differences in terms of source contributions or external parameters correlations (ie. eBC) between the 5 factors unoptimized solution and the optimized one? In others words, are the differences significant?*

**Response:** We thank the reviewer for a very constructive remark. The differences between the PMF and optimized solutions are indeed significant, especially in terms of relative contributions of the different sources. Specifically, COA and HOA are significantly lower in the optimized solution. The paragraph where the unconstrained and constrained solutions are compared has been modified in the revised manuscript to include a comparison between the relative contributions and the correlations with externals for the unconstrained and optimized solutions. An additional figure with the comparison of the relative contributions has been added in the supplementary information and table S1 has been modified to include the correlation parameters for the PMF solution.

#### **Changes in text:**

Compared to the unconstrained solution (average over 10 seeds), the optimized solution (average over all good *a* value combinations) has more genuine factor profiles (Fig. 3), with decreased contributions of *m/z* 60 in the HOA spectra (from 0.009 ± 0.001% to 0.003 ± 0.001%) and of *m/z* 44 in the COA spectra (from 0.069 ± 0.001% to 0.013 ± 0.002%). **In terms of the relative contributions of the different sources to the total OA (Fig. S7), the optimized solution yielded significantly lower COA (7.0 ± 1.1 % vs. 19.9 ± 0.1% in the unconstrained PMF) and HOA (15.1 ± 1.6 % vs. 25.1 ± 0.1% in the unconstrained PMF).** Moreover,  $\sigma_{\text{ALL}}$ , **the object function that we seek to minimize**, decreases considerably from 3.3 ± 0.1 in the unconstrained solution to 1.0 ± 0.1 in the optimized solution. In terms of the model mathematical performance, there is only a moderate increase in the residuals in the optimized solution compared to the unconstrained run. Specifically, *Q* normalized by its expected value (*Q/Q<sub>exp</sub>*) (Paatero and Hopke, 2009)

increases from  $7.5 \pm 0.1$  in the unconstrained solution to  $8.5 \pm 0.4$  in the optimized solution. The correlations between the OA factors from the optimized solution and its corresponding tracers are presented in Fig. S7. [and the correlation parameters \( \$R^2\$  and slope\) are reported in Table S1.](#) The correlation parameters ( $R^2$  and slope) are reported in Table S1 for the unconstrained and optimized solutions. Compared to the unconstrained solution, the correlations between COA and its marker ( $C_6H_{10}O$ ) are higher in the optimized solution, while the correlations between OOA and  $NH_4$  are slightly lower in this case, especially during the haze events.

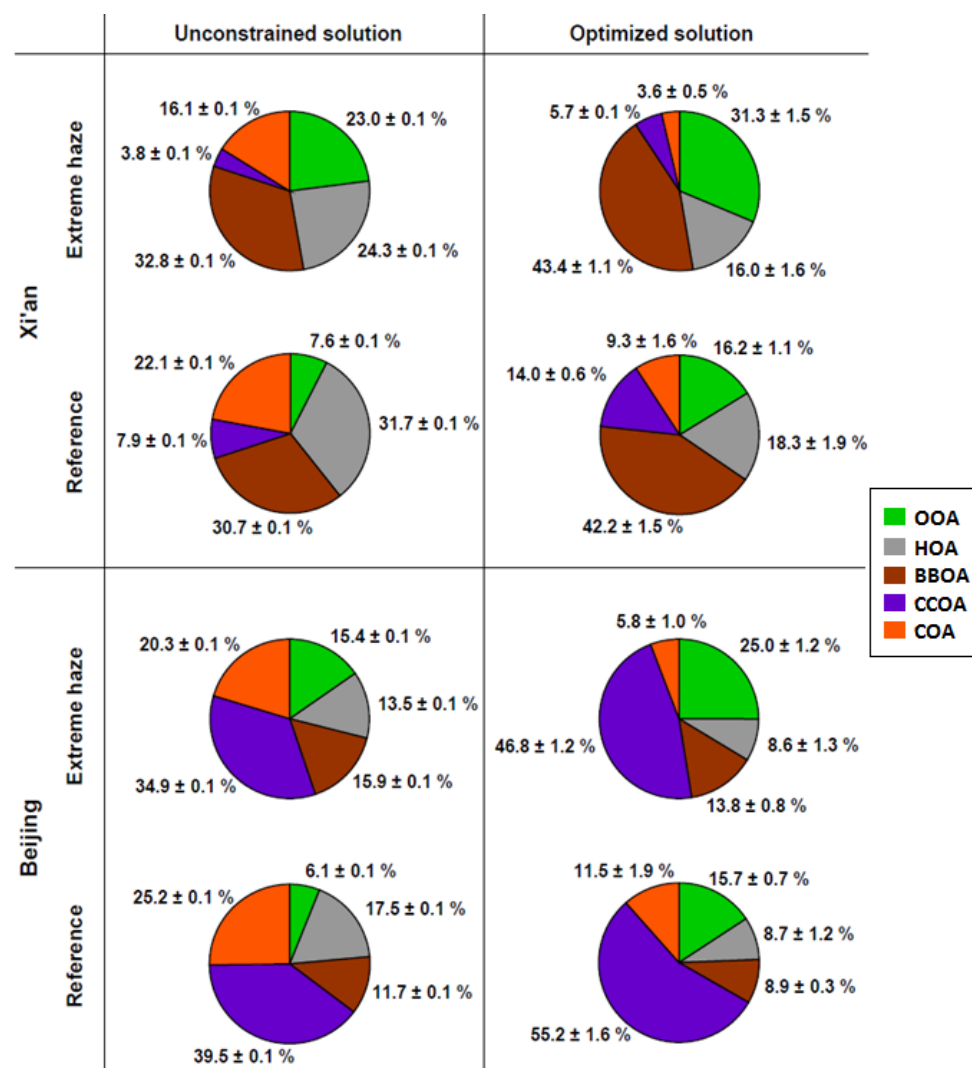


Figure S7 (NEW): Comparison of the unconstrained and optimized solutions in terms of the relative contributions of the OA sources for the four periods of interest.

Table S1 (MODIFIED): Squared Pearson coefficient (top) and ratios (bottom) derived from the correlations between the OA sources and its external time series for the four periods of interest as represented in Fig. S7. **The values reported in parenthesis are related to the unconstrained source apportionment solution (average of 10 runs).**

R <sup>2</sup>	Xi'an		Beijing		Overall
	Extreme haze	Reference	Extreme haze	Reference	
OOA vs. NH <sub>4</sub>	0.22 (0.50)	0.71 (0.83)	0.38 (0.63)	0.60 (0.53)	0.88 (0.92)
COA vs. C <sub>6</sub> H <sub>10</sub> O	0.21 (0.008)	0.58 (0.29)	0.44 (0.2)	0.71 (0.53)	0.31 (0.39)
CCOA vs. PAH	0.57 (0.61)	0.59 (0.60)	0.96 (0.97)	0.96 (0.97)	0.62 (0.63)
BBOA vs. C <sub>2</sub> H <sub>4</sub> O <sub>2</sub>	0.98 (0.96)	0.96 (0.88)	0.79 (0.80)	0.81 (0.78)	0.97 (0.96)
BBOA vs. eBC <sub>wb</sub>	0.33 (0.34)	0.53 (0.53)	N.A.	N.A.	0.38 (0.38)
HOA vs. eBC <sub>tr</sub>	0.61 (0.67)	0.61 (0.62)	N.A.	N.A.	0.61 (0.63)

Ratio (source/marker)	Xi'an		Beijing		Overall
	Extreme haze	Reference	Extreme haze	Reference	
OOA/NH <sub>4</sub>	0.99 (0.74)	1.08 (0.64)	0.67 (0.42)	0.76 (0.31)	0.97 (0.70)
COA/C <sub>6</sub> H <sub>10</sub> O	60 (219)	144 (267)	126 (372)	198 (304)	96 (243)
CCOA/PAH	3.4 (2.4)	5.5 (3.3)	10.8 (8.4)	10.4 (7.9)	7.2 (5.2)
BBOA/C <sub>2</sub> H <sub>4</sub> O <sub>2</sub>	51 (39)	54 (39)	29 (34)	22 (28)	51 (39)
BBOA/eBC <sub>wb</sub>	10.8 (8.3)	4.9 (3.6)	N.A.	N.A.	7.3 (5.5)
HOA/eBC <sub>tr</sub>	1.18 (0.62)	1.6 (2.6)	N.A.	N.A.	1.27 (0.63)

**P30141 line 15 and 22.** HOA and COA profiles used to constrain the ME2 model were obtained in Paris with an unconstrained PMF approach. Can you add few words discussing the representativity of those source profiles considering that the vehicular fleet is potentially significantly different as well as cooking activities (despite the COA profile was obtained in the Paris Chinatown). The use of a values allows to minimize this potential issue of representativity of the source profile, but here I'll provide more information about how the use of a values improved this representativity under the light of the results obtained with the unoptimized solution.

**Response:** We fully agree with the reviewer that this point should be discussed in more detail. Therefore, we used cosines similarity analysis to compare various HOA and COA profiles from different regions. Given two vectors with n elements (A<sub>i</sub> and B<sub>i</sub>, with i=1,2..n), the cosine similarity is defined as:

$$\text{cosine similarity} = \frac{\sum_{i=1}^n A_i \cdot B_i}{\sqrt{\sum_{i=1}^n (A_i)^2} \cdot \sqrt{\sum_{i=1}^n (B_i)^2}}$$

The cosine similarity analysis can result in values between -1 and 1, with 1 indicating a coincident vector, and 0 representing orthogonality. Our results show that the use of European HOA and COA profiles is adequate for China, as these two profiles are found to be little variable for different environments (i.e. similar HOA in the United states and Europe and similar COA in Europe and China).

## Changes in text:

To decrease the influence of BBOA on the apportionment of HOA, we constrained HOA using the profile from Crippa et al. (2013), which is characterized by a minor contribution of  $m/z$  60. Note that while other approaches were explored throughout the entire analysis, including the use of other HOA profiles or increase of the factor number, the BBOA-HOA separation couldn't be significantly improved. **As the vehicular fleet in China and Europe are significantly different, - e.g. higher diesel contribution in Europe, the use of a European profile to apportion traffic emissions in China could introduce significant errors. However, the comparison between HOA spectra from Europe (fleet dominated by diesel) and from the United states (fleet dominated by gasoline), shows that the variability among two European spectra (Mohr et al., 2012 and Crippa et al., 2013) is comparable to the variability among HOA spectra from the United States and Europe (Docherty et al., 2011 and Crippa et al., 2013). This was evaluated by means of cosine similarity analysis, which resulted in  $\Theta_{\text{HOA(Europe-Europe)}} = 0.93$  and  $\Theta_{\text{HOA(Europe-US)}} = 0.92$ . Thus, we show that HOA emissions from different types of cars have similar profiles.** Although constraining the HOA profile improves the HOA-BBOA separation, it compromises the apportionment of cooking emissions, with a higher background mass and unexpectedly high concentration overnight in the diurnal trend. To avoid the mixing of COA with other sources, the COA profile of Crippa et al. (2013) was constrained. **While some differences are expected between the Chinese and European cooking activities, cosines similarity analysis indicate very good correlations ( $\Theta_{\text{COA(Europe-China)}} = 0.97$  on average) between the COA profile from Paris and four spectra from different types of Chinese cooking (CC1 to CC4 in He et al., 2010). Moreover, the use of  $\alpha$ -values allows for a certain re-adjustment of the input profiles (for both HOA and COA), minimizing the effect of using a non-local input profiles.** In the following we discuss the sensitivity of the results to the  $\alpha$  values used to constrain the HOA and COA factor profiles.

**P30145 line 25.** *This information ("analyses were conducted separately for the four periods") should be given at the beginning of this section. I assume that the discussion and the illustrations (fig 1, 2 and 3) related to the solutions optimization is for one of the period. Specify which one or clarify. Also the haze period in Beijing is really short, do you observe any discontinuity with the non-haze period?*

## Response:

The source apportionment optimization (Fig 1,2,3) was performed using the full dataset, while all the following results (e.g. relative contributions, correlations with externals...) are presented separately for the four periods. The following sentence: "These analyses were conducted separately" refers only to the correlations between the OA factors and external parameters discussed in the previous sentence. This sentence has been removed to avoid confusion.

The extreme haze period in Beijing contains two short time periods (with a small gap of some hours), with a total of 28 hours of extreme haze. At the beginning of the extreme haze events there is a steep increase in the  $\text{PM}_{2.5}$  mass (Fig 1) in correspondence with an increase in the RH. Moreover the extreme haze in Beijing shows similar characteristics than Xi'an: bigger particles, increased fraction of inorganics and OOA, etc.

**P30147 line 27.** *A standard deviation can be considered as an error only if we expect equal values (which is not the case here).*

**Response:** We agree; "as errors" has been removed.

**P30148 line3.** *True considering absolute concentrations, but the relative contribution of  $\text{NH}_4$  decrease during haze events. How about the ionic balance? In such environments and conditions, acidic properties of aerosol is of great interest (SOA formation pathways etc.).*

**Response:** We decided not to report the ionic balance due to the large uncertainties that this method has for determining the acidic properties of the aerosols. In our case, one of the major issues is the presence of primary Cl emissions, which in Xi'an was observed as big peaks (up to  $100 \mu\text{g m}^{-3}$ ) in the time series. The Cl time series correlates with the major Zn isotopes (see Fig R2). Therefore, we assume part of the measured Cl to be emitted in the form of ZnCl from industrial zincification processes. Moreover, also primary emissions of organochlorides from combustion emissions are expected. As shown in Fig R3, the Cl

mass has an important effect on the ionic balance, which shows acidic properties when Cl is included (i.e. all Cl as secondary) and fully neutralized aerosol if Cl is not included (i.e. all Cl is assumed to be primary).

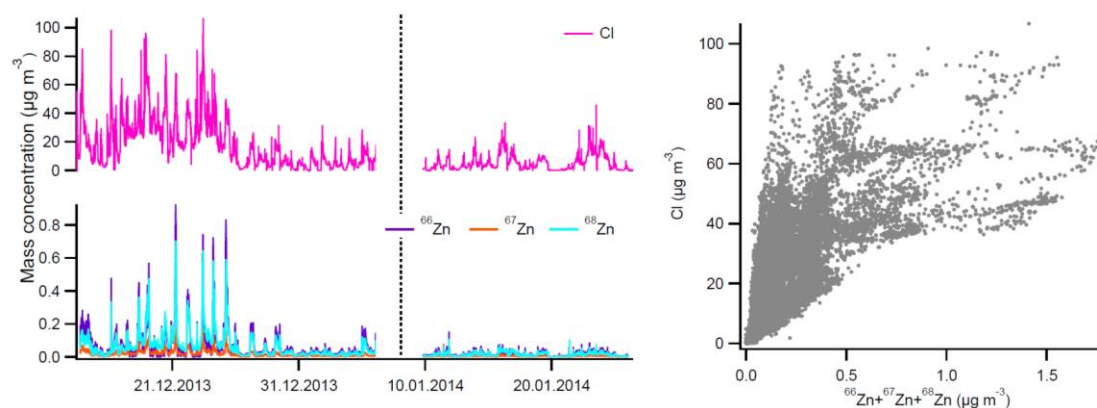


Figure R2: Left: Time series of Cl (upper pannel) and major Zn isotopes (lower pannel) over the full measurement period; Right: Scatter plot between Cl and sum of the major Zn isotopes over the full time series

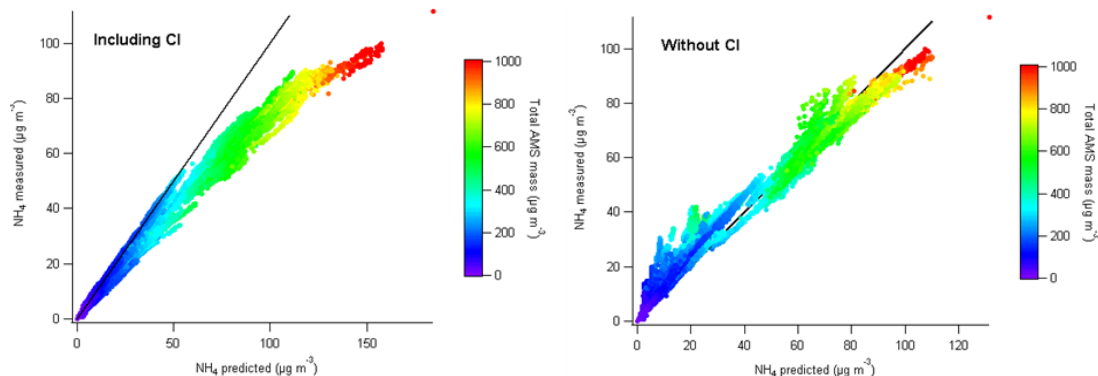


Figure R3:  $\text{NH}_4$  measured vs predicted from ionic balance by using all the inorganic compounds (left) or neglecting the Cl (right).

Another issue can be related to the presence of organo-nitrates and organo-sulfates that respond in the AMS as nitrate and sulfate. The presence of such species represents a small interference for the reported sulfate and nitrate mass and therefore also to the ionic balance, making the aerosol appear more acidic.

**P30152-P3053.** Not sure that evolutions of the absolute concentrations or contributions vs RH are useful here. From the results presented here it seems that the aerosol acidity strongly increase during haze periods. I suggest to add the ionic balance of the aerosol in figure 8b. Also such conditions (high RH, high  $\text{SO}_4$  and very high OA concentrations) are ideal to have a careful look to the organo-sulfur fragments. Do you observe any of those specific fragments during the field campaign and especially during haze periods?

#### Response:

As explained in the previous comment we decided not to report the ionic balance because of the large uncertainties related to these analyses.

Regarding the organo-sulfate fragments, the only sulfur containing fragment that we could unambiguously fit in the HR was  $\text{CH}_3\text{SO}_2$ . This fragment is usually related to methanesulfonic acid (MSA) from marine aerosols. However, our backtrajectory analyses don't indicate any marine influence in the sampling sites during the measurement period. Another possibility is that this fragment derives from organo-sulfates. As shown in Fig. R4, the  $\text{CH}_3\text{SO}_2$  follows the time series of OOA. This high correlation could be an indication that a certain fraction of our OOA might be related to organo-sulfates. However, the origin of this fragment is not certain and we don't have any external measurements to prove that it's related to organo-sulfates. As previously mentioned, the presence of such fragments represents a small interference for the reported sulfate mass (and therefore to the ionic balance).

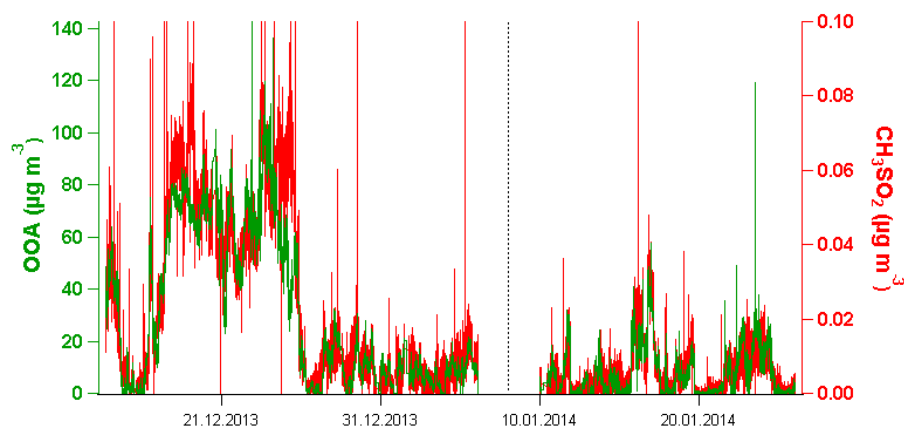


Figure R4: OOA and  $\text{CH}_3\text{SO}_2$  time series for the full measurement period.

**P30154 PAH sources.** As stated above the PAH concentrations reported here are very high. A rough calculation shows that PAHs contribute to few % of the OA mass concentration (1-5%) which is really high (!). In Europe or US, PAHs contribution to OA is typically in the range 0.01-0.1 % maximum. It seems also that the PAH contribution to OA is much higher in Beijing than in Xi'an, most probably due to coal emissions. I suggest to the authors to put the PAH concentration and/or PAH contribution to OA into perspective with literature data (ambient and source). I guess, it isn't possible to extract the PAH signatures ( $f(m/z)$ ) of the different sources (traffic, coal and BB) from your analysis. But if I'm wrong, this information could be very interesting.

#### Response:

We agree with the reviewer that the PAH to OA ratios that we find (AMS-PAH/OA of  $1.9 \pm 0.7$  % in Xi'an and  $4.4 \pm 2.2$  % in Beijing) are higher than the ones commonly reported for Europe and the US. There are two main reasons that can explain this difference: the different methodologies to measure PAHs and the different contributions of PAH-emitting sources to total OA. Regarding the PAH measurement techniques, as already mentioned, previous work have shown that PAH quantified from AMS measurements are systematically higher than PAH determined from filter measurements (Bruns et al., 2015). As we have discussed above, filter sampling might be associated with negative artefacts related to the volatilization of semi-volatile PAHs and the oxidation of unstable PAHs. On the other hand, the methodology adapted here would yield highest estimates of PAHs' concentrations, due to the use of a low RIE and potential interferences from non-PAHs compounds that are present in combustion emissions (i.e. PAHs only correlate with POA). Unfortunately, we do not have access to the filter samples for offline analysis of the PAHs and we believe that comparisons between offline and online methodologies require dedicated and systematic work. For this reasons, we will refer to the PAHs in the manuscript as AMS-PAHs, which should be considered as absolute highest estimates. In terms of the contributing sources, in our case combustion sources, especially coal burning, explain a very large fraction of OA, which would enhance the PAH to OA ratio compared to Europe. Chen et al., (2005) reported mean PAH/OC of 28 % (i.e. PAH/OA of 17.5 % assuming OA/OC of 1.6) for bituminous coal and 0.8 % (i.e. PAH/OA of 0.5 %) for anthracite from filter measurements. Considering that a mixture of these two types of coal is used in the cities considered in this work and that the relative contribution of coal to the total OA is higher in Beijing than in Xi'an, the obtained AMS-PAH/OA ratios seem reasonable. We didn't find very significant differences between the AMS-PAH spectra observed in Beijing and Xi'an, where different emission sources prevail, indicating that PAHs from different sources have similar profiles.

#### Changes in text:

Page 30154, Line 18: The high AMS-PAH concentrations lead to high AMS-PAH to OA ratios ( $1.9 \pm 0.7$  % in Xi'an and  $4.4 \pm 2.2$  % in Beijing) compared to previous reported values for Europe. This can be related to the different methodologies used to measure PAHs (e.g. volatilization of semi-volatile PAHs and oxidation of unstable PAHs on filters). Moreover, in our case combustion sources, especially coal burning, explain a very large fraction of OA, which would enhance the AMS-PAH to OA ratio compared to Europe. In this regard, Chen et al., (2005) reported mean PAH to OC ratios of 28 % (i.e. PAH/OA of 17.5 % assuming OA/OC of 1.6) for bituminous coal and 0.8 % (i.e. PAH/OA of 0.5 %) for anthracite. Considering that a mixture of these two types of coal is used in the cities considered in this work and that the relative contribution of coal to the total OA is higher in Beijing than in Xi'an, the obtained AMS-PAH to OA ratios seem reasonable.

**P30156 line9-11:** This sentence is apparently in contradiction with the sentence P30145 line 25 (“analyses were conducted separately for the four periods”)

**Response:** As previously mentioned, the source apportionment optimization was performed using the full dataset, while all the following results (e.g. relative contributions, correlations with externals...) are presented separately for the four periods.

**Figure 4.** I'd add the visibility shown in fig S9.

**Response:** Added in revised manuscript

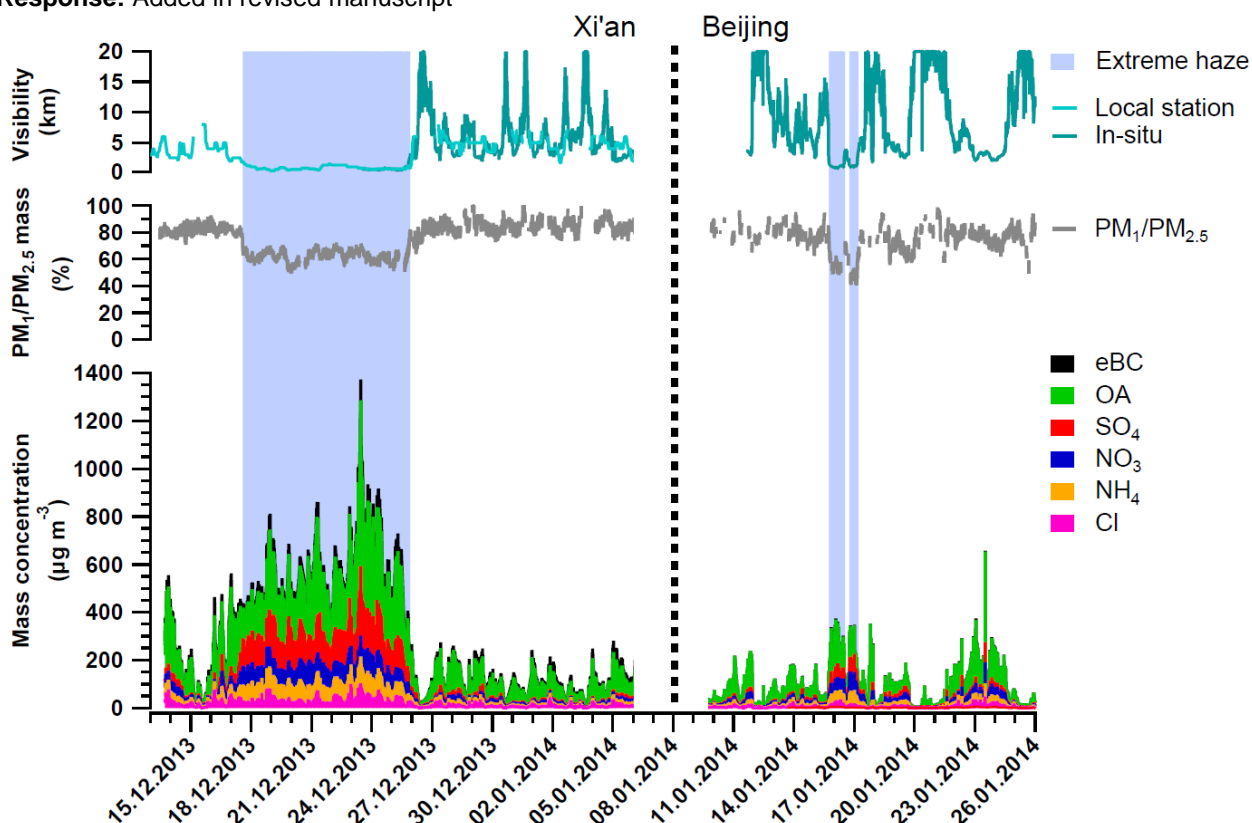


**Fig 6 (A):** Difficult to see the comparisons with “external” parameters. Try to make these figs clearer.

**Response:** We enlarged Fig.6A in the revised manuscript to improve the visualization of the comparisons with the external parameters.

**Fig6 (B)** Add the total OA concentration above each pie chart

**Response:** Added in the revised manuscript.

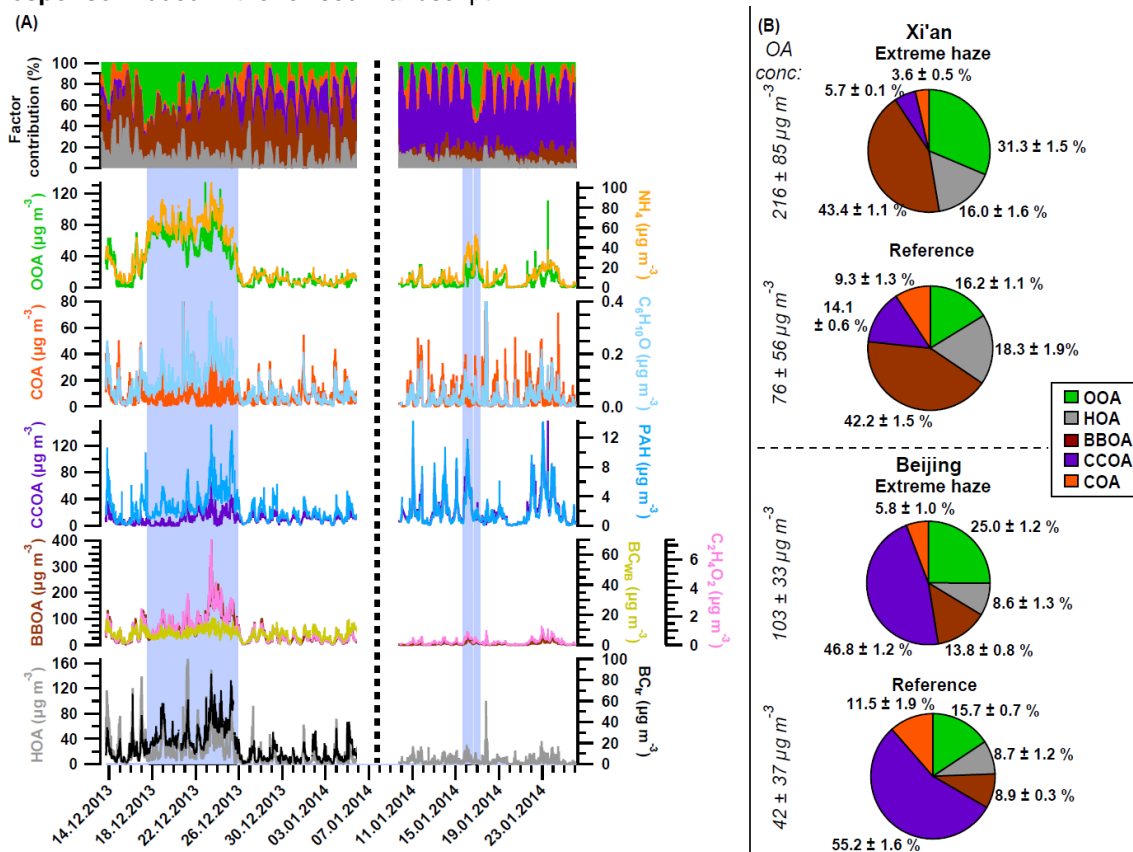


**Fig 7** Legend not readable in my printed version

**Response:** Bigger in revised manuscript

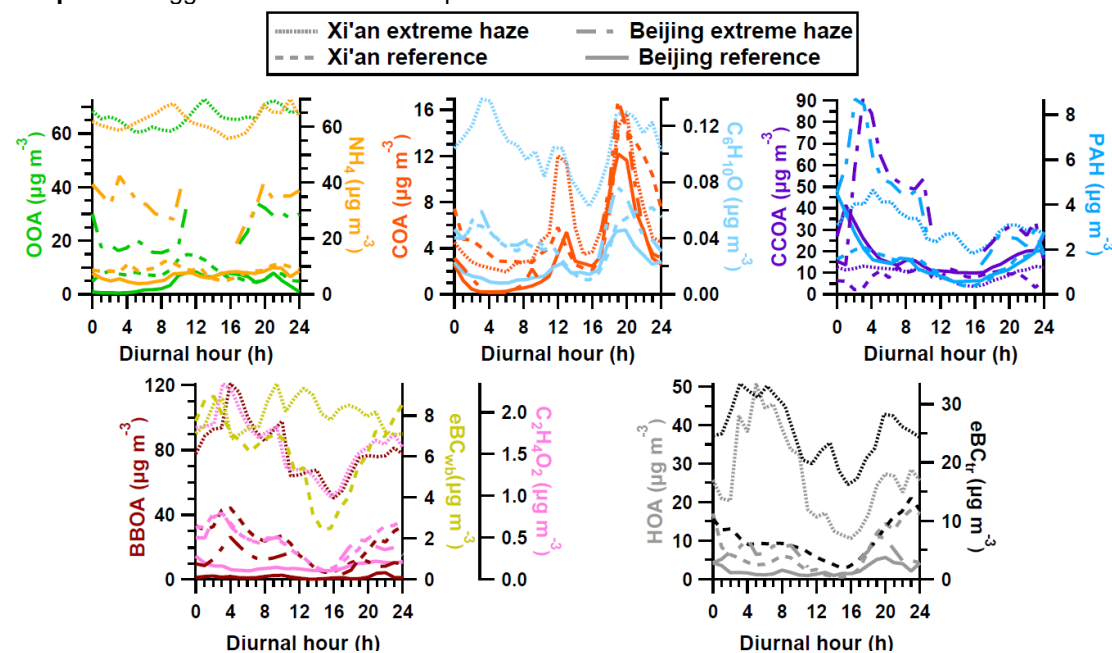
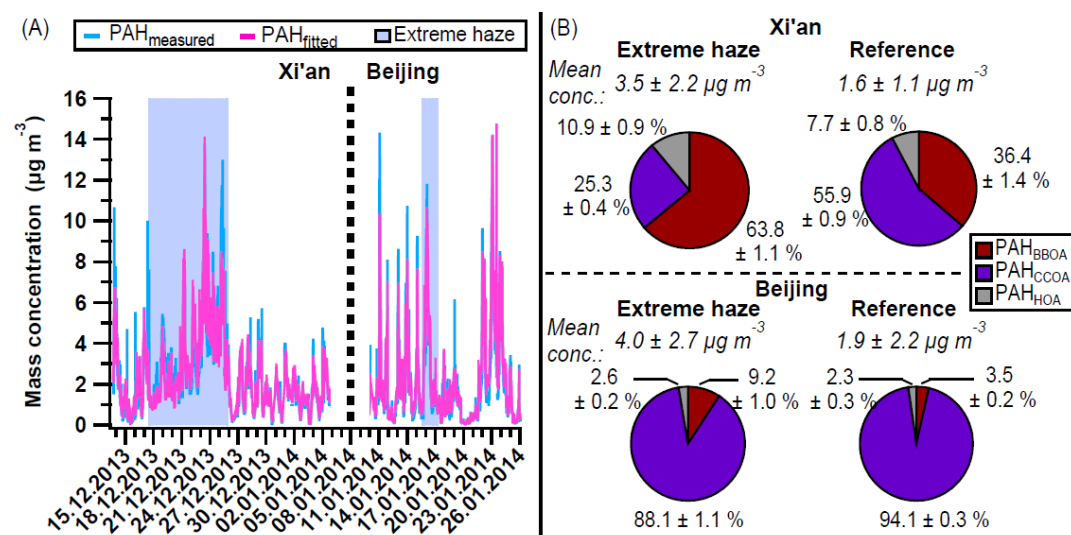


**Fig 10B** Add the total PAH concentration above each pie chart.

**Response:** Added in the revised manuscript.



In the SI or in the main text, I'd add a table summarizing all relevant concentrations (OA, NO<sub>3</sub>, SO<sub>4</sub>, NH<sub>4</sub>, BC, HOA, BBOA, CCOA, COA, OOA, PAH, ..).

**Response:** A table with all the average concentrations has been added in the supplementary information.

**Table S2 (New): Mean concentration and standard deviation for all measured compounds and sources for the four periods of interest.**

Mean conc. ( $\mu\text{g m}^{-3}$ )	Xi'an		Beijing	
	Extreme haze	Reference	Extreme haze	Reference
PM <sub>2.5</sub>	537 ± 146	140 ± 99	243 ± 47	75 ± 61
OA	216 ± 85	76 ± 56	103 ± 33	42 ± 37
SO <sub>4</sub>	119 ± 30	12 ± 12	47 ± 15	12 ± 11
NO <sub>3</sub>	71 ± 12	14 ± 11	43 ± 11	7.4 ± 5.6
NH <sub>4</sub>	31 ± 15	11.4 ± 10.6	14.9 ± 5.1	5.3 ± 5.4
Cl	62 ± 12	11.3 ± 9.0	35.4 ± 7.9	8.4 ± 6.6
eBC	39 ± 16	15.0 ± 9.5	3.4 ± 1.1	1.5 ± 1.3
OOA	47 ± 12	5.4 ± 8.9	14.7 ± 5.5	2.4 ± 3.1
HOA	49 ± 41	23 ± 27	12.9 ± 9.0	6.9 ± 9.9
BBOA	67 ± 40	22 ± 20	15.1 ± 9.6	4.6 ± 6.9
CCOA	7.7 ± 8.0	5.7 ± 4.1	33 ± 23	16 ± 18
COA	33 ± 16	15.8 ± 8.7	19 ± 10	10.0 ± 9.6
PAH	3.5 ± 2.2	1.6 ± 1.1	4.0 ± 2.7	1.9 ± 2.2

**Changes in text:**

Page 30147, Line 7: **Table S2 contains a summary of the mean concentrations of all measured compounds and OA sources during the four time periods.**

References:

- Bente, M., Sklorz, M., Streibel, T., and Zimmermann, R.: Thermal Desorption-Multiphoton Ionization Time-of-Flight Mass Spectrometry of Individual Aerosol Particles: A Simplified Approach for Online Single-Particle Analysis of Polycyclic Aromatic Hydrocarbons and Their Derivatives, *Anal. Chem.*, 81, 2525–2536, 2009.
- Bruns, E. A., Krapf, M., Orasche, J., Huang, Y., Zimmermann, R., Drinovec, L., Močnik, G., El-Haddad, I., Slowik, J. G., Dommen, J., Baltensperger, U., and Prévôt, A. S. H.: Characterization of primary and secondary wood combustion products generated under different burner loads, *Atmos. Chem. Phys.*, 15, 2825–2841, 2015.
- Chen, Y., Sheng, G., Bi, X., Feng, Y., Mai, B., and Fu, J.: Emission factors for carbonaceous particles and polycyclic aromatic hydrocarbons from residential coal combustion in China, *Environ. Sci. Technol.*, 39, 1861–1867, 2005.
- DeWitt, H. L., Hellebust, S., Temime-Roussel, B., Ravier, S., Polo, L., Jacob, V., Buisson, C., Charron, A., André, M., Pasquier, A., Besombes, J. L., Jaffrezo, J. L., Wortham, H., and Marchand, N.: Near-highway aerosol and gas-phase measurements in a high-diesel environment, *Atmos. Chem. Phys.*, 15, 4373–4387, 2015.
- Dzepina, K., Arey, J., Marr, L. C., Worsnop, D. R., Salcedo, D., Zhang, Q., Onasch, T. B., Molina, L. T., Molina, M. J., and Jimenez, J. L.: Detection of particle-phase polycyclic aromatic hydrocarbons in Mexico City using an aerosol mass spectrometer, *Int. J. Mass Spectrom.*, 263, 152–170, 2007.
- Eriksson, A. C., Nordin, E. Z., Nyström, R., Pettersson, E., Swietlicki, E., Bergvall, C., Westerholm, R., Boman, C., and Pagels, J. H.: Particulate PAH Emissions from Residential Biomass Combustion: Time-Resolved Analysis with Aerosol Mass Spectrometry, *Environ. Sci. Technol.*, 2014, 48, 7143–7150, 2014.
- Gentner, D. R., Jathar, S. H., Gordon, T. D., Bahreini, R., Day, D. A., El Haddad, I., Hayes, P. L., Platt, S. M., Pieber, S. M., de Gouw, J., Goldstein, A. H., Harley, R. A., Jimenez, J. L., Prévôt, A. S. H., and Robinson, A. L.: Contribution of gasoline and diesel motor vehicles to secondary organic aerosol formation in urban areas worldwide: a review, *In prep.*
- He, L.-Y., Lin, Y., Huang, X.-F., Guo, S., Xue, L., Su, Q., Hu, M., Luan, S.-J., and Zhang, Y.-H.: Characterization of high-resolution aerosol mass spectra of primary organic aerosol emissions from Chinese cooking and biomass burning, *Atmos. Chem. Phys.*, 10, 11535–11543, 2010.
- Linstrom, P.J., and Mallard, W.G. (Eds.): NIST Chemistry WebBook, NIST standard reference database number 69, National Institute of Standards and Technology, Gaithersburg MD, 20899, <http://webbook.nist.gov>, last access 2 February 2016.